

# Investigation of large $\alpha$ production in reactions involving weakly bound ${}^7\text{Li}$

S. K. Pandit,<sup>1,2,\*</sup> A. Shrivastava,<sup>1,2</sup> K. Mahata,<sup>1,2</sup> V. V. Parkar,<sup>1</sup> R. Palit,<sup>3</sup> N. Keeley,<sup>4</sup> P. C. Rout,<sup>1,2</sup> A. Kumar,<sup>1</sup> K. Ramachandran,<sup>1</sup> S. Bhattacharyya,<sup>5</sup> V. Nanal,<sup>3</sup> C. S. Palshetkar,<sup>3</sup> T. N. Nag,<sup>6</sup> Shilpi Gupta,<sup>1,2</sup> S. Biswas,<sup>3</sup> S. Saha,<sup>3</sup> J. Sethi,<sup>3</sup> P. Singh,<sup>3</sup> A. Chatterjee,<sup>1</sup> and S. Kailas<sup>1</sup>

<sup>1</sup>*Nuclear Physics Division, Bhabha Atomic Research Centre, Mumbai - 400085, India*

<sup>2</sup>*Homi Bhabha National Institute, Anushaktinagar, Mumbai - 400094, India*

<sup>3</sup>*Department of Nuclear and Atomic Physics, Tata Institute of Fundamental Research, Mumbai 400005, India*

<sup>4</sup>*National Centre for Nuclear Research, ul. Andrzeja Soltana 7, 05-400 Otwock, Poland*

<sup>5</sup>*Variable Energy Cyclotron Centre, Kolkata - 700064, India*

<sup>6</sup>*Radiochemistry Division, Bhabha Atomic Research Centre, Mumbai - 400085, India*

(Received 16 August 2017; published 19 October 2017)

The origin of the large  $\alpha$ -particle production cross sections in systems involving weakly bound  ${}^7\text{Li}$  projectiles has been investigated by measuring the cross sections of all possible fragment-capture as well as complete fusion using the particle- $\gamma$  coincidence, in-beam, and off-beam  $\gamma$ -ray counting techniques for the  ${}^7\text{Li} + {}^{93}\text{Nb}$  system at near Coulomb barrier energies. Almost all of the inclusive  $\alpha$ -particle yield has been accounted for. While the  $t$ -capture mechanism is found to be dominant ( $\sim 70\%$ ), compound nuclear evaporation and breakup processes contribute  $\sim 15\%$  each to the inclusive  $\alpha$ -particle production in the measured energy range. Systematic behavior of the  $t$  capture and inclusive  $\alpha$  cross sections for reactions involving  ${}^7\text{Li}$  over a wide mass range is also reported.

DOI: [10.1103/PhysRevC.96.044616](https://doi.org/10.1103/PhysRevC.96.044616)

## I. INTRODUCTION

Investigation of the mechanisms responsible for the large inclusive  $\alpha$ -particle production cross sections observed in systems involving weakly bound projectiles with  $\alpha + x$  cluster structure, e.g.,  ${}^6,{}^8\text{He}$ ,  ${}^6,{}^7\text{Li}$ , and  ${}^7,{}^9\text{Be}$ , compared to that of the complementary fragments is of current interest [1–5]. Different reaction mechanisms, e.g., breakup (direct and sequential), nucleon transfer followed by breakup, cluster transfer, incomplete fusion (only part of the projectile fuses), and compound nuclear (CN) evaporation, contribute to the  $\alpha$  yield. It is difficult to separate the contributions of these individual reaction mechanisms from an inclusive  $\alpha$ -particle spectrum. Exclusive measurements are therefore needed to investigate the origins of the large  $\alpha$  production and to study the role of the weakly bound cluster structure in the reaction dynamics.

The present work aims to study the sources of the large  $\alpha$  yields for reactions induced by  ${}^7\text{Li}$  nuclei by extensive measurements of different reaction channels. Most of the data for  ${}^7\text{Li}$  are for inclusive  $\alpha$  cross sections [1,2]. Also, simultaneous measurements of all processes leading to  $\alpha$  particles in the outgoing channel are not available for the same system. In our recent work on the  ${}^7\text{Li} + {}^{93}\text{Nb}$  system [6], contributions to the  $\alpha$  yield originating from the breakup of  ${}^7\text{Li}$  ( ${}^7\text{Li}^* \rightarrow \alpha + t$ ) together with  $1p$  pickup followed by breakup ( ${}^8\text{Be} \rightarrow \alpha + \alpha$ ) and  $1n$  stripping followed by breakup ( ${}^6\text{Li} \rightarrow \alpha + d$ ) were disentangled by performing exclusive measurements. The sum of these cross sections could account for only  $\sim 8\%$  of the inclusive  $\alpha$  yield. To understand the remaining part, we have now extended the cross section measurements of  $\alpha$  producing channels to the  $t$  stripping and/or capture reaction, which was suggested as one of the main sources of  $\alpha$ -particle production in Ref. [6].

This paper reports measurements of prompt  $\gamma$  rays in coincidence with  $\alpha$  particles in the outgoing channels to identify the dominant reaction mechanism contributing to the  $\alpha$ -particle production for the  ${}^7\text{Li} + {}^{93}\text{Nb}$  system near Coulomb barrier energies. The absolute cross sections of residues arising from  $t$  capture were extracted by measuring the characteristic  $\gamma$ -ray transitions employing the in-beam and off-beam  $\gamma$ -ray counting methods. The two processes,  $t$  capture after breakup of  ${}^7\text{Li}$  and direct  $t$  stripping, are difficult to separate experimentally, although it has been reported that the  $t(d)$ -capture reaction dominates over one-step stripping for  ${}^7\text{Li}({}^6\text{Li})$  projectiles [7–10]. In this work, the mixture of these two processes is referred to as  $t$  capture. The  $2n$ -stripping channel, contributing to the  $\alpha$  particle yield via breakup of the unbound  ${}^5\text{Li}$ , has also been obtained by counting the  $\gamma$  rays corresponding to radioactive decay of  ${}^{95}\text{Nb}$ . The cross sections of residues from complete fusion were measured to optimize the statistical model parameters used to predict the  $\alpha$ -evaporation probability. The  $\alpha$ -capture cross sections were also measured to compare with those for  $t$  capture. A systematic study of the  $t$ -capture and inclusive  $\alpha$  cross sections for reactions involving  ${}^7\text{Li}$  on various targets over a wide mass range has also been performed.

The paper is organized as follows. Experimental details are given in Sec. II. The analysis and results are presented in Sec. III. Details of the statistical model calculations for compound nuclear decay and distorted wave Born approximation (DWBA) calculations are described in Sec. IV. A systematic study of  $t$ -capture and  $\alpha$ -particle production cross sections is discussed in Sec. V followed by a summary and conclusions in Sec. VI.

## II. EXPERIMENTAL DETAILS

Two independent experiments were carried out for in-beam and off-beam  $\gamma$ -ray counting, using the  ${}^7\text{Li}$  beam from the

\*sanat@barc.gov.in

Pelletron-Linac facility, Mumbai. Both measurements were performed at beam energies of 24, 26, 28, and 30 MeV, some of which are common to the previous measurement of breakup fragments in coincidence [6]. Self-supporting  $^{93}\text{Nb}$  foils of thickness  $\sim 1.6 \text{ mg/cm}^2$  were used as targets.

Prompt  $\gamma$ -ray transitions were detected using the Indian National Gamma Array (INGA) [11], consisting of 18 Compton suppressed high purity germanium (HPGe) clover detectors. In this particular array configuration the detectors were arranged at six different angles with three detectors each at  $\pm 40^\circ$ ,  $-65^\circ$ , and  $-23^\circ$ , two detectors at  $+65^\circ$  and four detectors at  $90^\circ$ . Three Si surface barrier telescopes (thicknesses  $\Delta E \sim 15\text{--}30 \mu\text{m}$ ,  $E \sim 300\text{--}5000 \mu\text{m}$ ), were placed inside the scattering chamber at  $35^\circ$ ,  $45^\circ$ , and  $70^\circ$  for the detection of charged particles around the grazing angle. One Si surface barrier detector (thickness  $\sim 300 \mu\text{m}$ ) was fixed at  $20^\circ$  to monitor Rutherford scattering for absolute normalization purposes. The time stamped data were collected using a digital data acquisition system with a sampling rate of 100 MHz [11]. Efficiency and energy calibration of the clover detectors was carried out using standard calibrated  $^{152}\text{Eu}$  and  $^{133}\text{Ba}$   $\gamma$ -ray sources.

The off-line  $\gamma$ -ray counting was carried out using an efficiency calibrated high-purity germanium (HPGe) detector. Low background was achieved by using graded shielding (Cu, Cd sheets of thickness  $\sim 2 \text{ mm}$  each followed by 5 cm of Pb). Aluminum catcher foils of thickness  $\sim 1 \text{ mg/cm}^2$  were used together with each target foil to stop the recoiling residues. The target and catcher foil assemblies were irradiated for  $\sim 6 \text{ h}$  (beam current  $\sim 50 \text{ nA}$ ) at each bombarding energy and counted together at a distance of 10 cm from the detector. A CAMAC scaler which recorded the integrated current in intervals of 1 min duration was used to monitor beam current.

### III. ANALYSIS AND RESULTS

A typical in-beam  $\gamma$ -ray add-back spectrum is shown in Fig. 1(a). The residues populated by  $t$  capture, complete fusion (CF), and nucleon transfer identified by detecting their characteristic  $\gamma$  rays are labeled. The  $\alpha$ -particle gated  $\gamma$ -ray spectrum shown in Fig. 1(b) gives a snapshot of the major reaction processes contributing to the  $\alpha$ -particle yield. The relative yields of  $\gamma$ -ray transitions from the residues of  $t$  capture ( $^{94,95}\text{Mo}$ ) are found to be greater than the others. The other reaction mechanisms contributing to the  $\alpha$  yields, namely,  $1p$  pickup ( $^7\text{Li}, ^8\text{Be} \rightarrow \alpha + \alpha$ )  $^{92}\text{Zr}$ , inelastic excitation ( $^7\text{Li}, ^7\text{Li}^* \rightarrow \alpha + t$ )  $^{93}\text{Nb}$ ,  $1n$  stripping ( $^7\text{Li}, ^6\text{Li}^* \rightarrow \alpha + d$ )  $^{94}\text{Nb}$ , and  $2n$  stripping ( $^7\text{Li}, ^5\text{Li} \rightarrow \alpha + p$ )  $^{95}\text{Nb}$  are also marked in the figure. An off-beam  $\gamma$ -ray spectrum is shown in Fig. 2 at a beam energy of 28 MeV.

#### A. $t$ -capture reaction

The cross sections for the residues from the  $t$ -capture mechanism,  $^{94,95}\text{Mo}$ , were obtained using the prompt  $\gamma$ -ray transitions shown in Fig. 1(a). For  $^{94}\text{Mo}$ , the yrast  $\gamma$ -ray transitions built on the ground state up to the  $J^\pi = 10^+$  excited state were considered [12]. The cross sections for  $^{95}\text{Mo}$  were obtained by adding the  $\gamma$ -ray transitions feeding directly to the ground state [13]. The  $^{93}\text{Mo}$  nucleus has a  $21/2^+$  isomeric state at  $E_{\text{ex}} =$

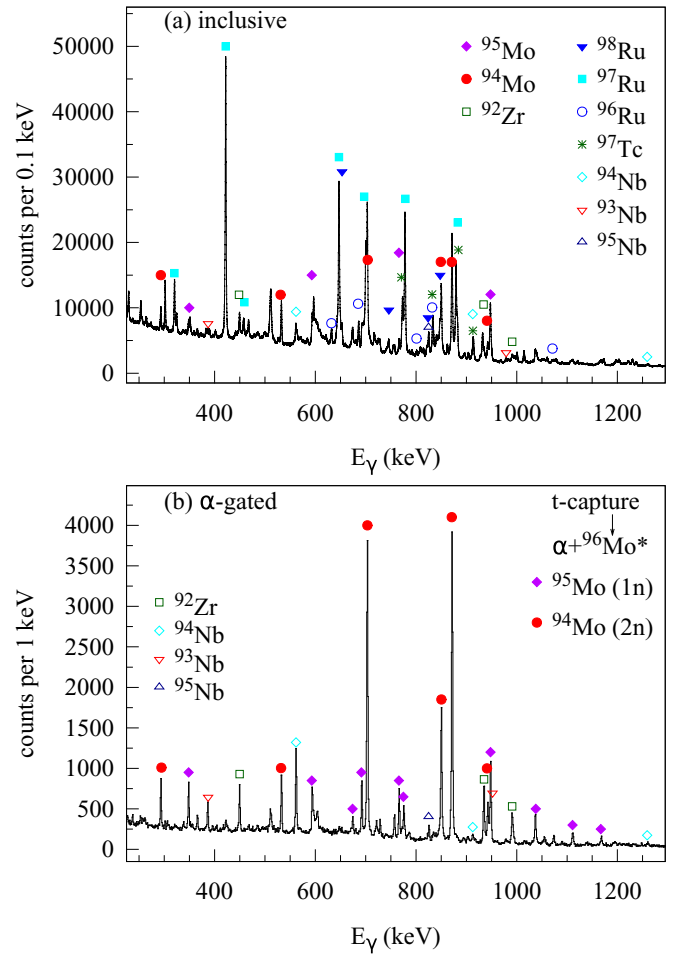


FIG. 1. A typical in-beam  $\gamma$ -ray spectrum for the  $^7\text{Li} + ^{93}\text{Nb}$  reaction at  $E_{\text{beam}} = 28 \text{ MeV}$ . (a) Inclusive spectrum with photopeaks from residues populated in the  $t$ -capture, CF, and nucleon transfer reaction processes marked. (b) Coincidence spectrum of  $\gamma$ -ray transitions with an  $\alpha$  particle selected as the outgoing fragment. The  $\gamma$ -ray transitions from  $^{94,95}\text{Mo}$  nuclei due to  $t$  capture followed by  $1n$  and  $2n$  evaporation are labeled. The photopeaks of  $\gamma$  rays from  $^{92}\text{Zr}$ ,  $^{93,94}\text{Nb}$ , and  $^{95}\text{Nb}$  formed by  $1p$  pickup followed by breakup ( $^8\text{Be} \rightarrow \alpha + \alpha$ ), inelastic excitation followed by breakup ( $^7\text{Li}^* \rightarrow \alpha + t$ ),  $1n$  stripping followed by breakup ( $^6\text{Li}^* \rightarrow \alpha + d$ ), and  $2n$  stripping followed by breakup ( $^5\text{Li} \rightarrow \alpha + p$ ), respectively are also labeled.

2.425 MeV with half-life  $T_{1/2} = 6.85 \text{ h}$ . The cross section for  $^{93m}\text{Mo}$  was obtained by following the radioactive decay of the isomeric state. The  $\gamma$ -ray transitions from the decay of  $^{93m}\text{Mo}$  can be seen in Fig. 2. The extracted cross sections for  $^{93\text{--}95}\text{Mo}$  are shown in Fig. 3(a). Sources of error on the data points are due to statistics,  $\gamma$ -ray detection efficiency, and available spectroscopic information of the residues. For off-beam measurements uncertainty in the target thickness was also included.

#### B. $\alpha$ -capture and $2n$ -stripping reactions

The  $\alpha$ -capture and  $2n$ -stripping mechanisms lead to  $^{95,96}\text{Tc}$  and  $^{95}\text{Nb}$ . These nuclei are radioactive with reasonable half-lives for decay from their ground states [ $T_{1/2}(^{95}\text{Tc}) = 20.0 \text{ h}$ ,

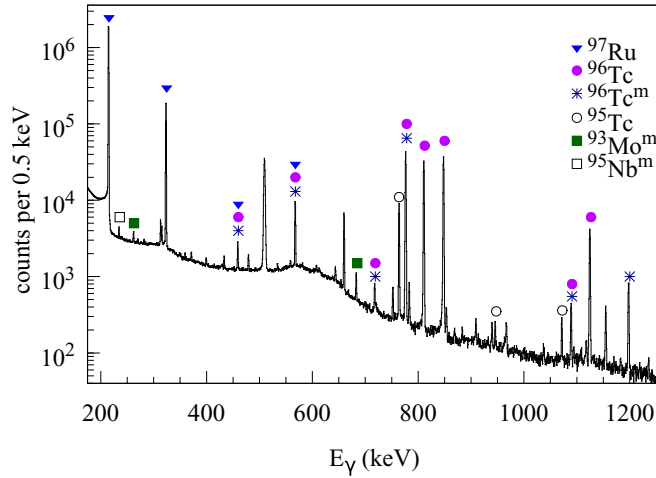


FIG. 2. A typical off-beam  $\gamma$ -ray spectrum for the  ${}^7\text{Li} + {}^{93}\text{Nb}$  reaction obtained after the end of the irradiation at  $E_{\text{lab}} = 28$  MeV for a counting time of 5 h. The  $\gamma$ -ray transitions from residues following CF ( ${}^{97}\text{Ru}$ ),  $\alpha$  capture ( ${}^{95,96}\text{Tc}$ ),  $t$  capture ( ${}^{93}\text{Mo}$ ), and  $2n$  transfer ( ${}^{95}\text{Nb}$ ) are labeled.

$T_{1/2}({}^{96}\text{Tc}) = 4.28$  d,  $T_{1/2}({}^{95}\text{Nb}) = 34.99$  d] as well as from metastable states [ $T_{1/2}({}^{95}\text{Tc}) = 61$  d,  $T_{1/2}({}^{96}\text{Tc}) = 51.5$  m,  $T_{1/2}({}^{95}\text{Nb}) = 3.61$  d]. The  $\gamma$ -ray transitions corresponding to decay of  ${}^{95,96}\text{Tc}$  and  ${}^{95}\text{Nb}$  are labeled in Fig. 2. The cross sections were extracted following the half-lives of each transition and are shown in Fig. 3(b).

### C. Complete fusion

The complete fusion of  ${}^7\text{Li}$  with  ${}^{93}\text{Nb}$  forms the compound nucleus (CN)  ${}^{100}\text{Ru}$ , which decays predominantly by neutron and proton emission. The characteristic prompt  $\gamma$ -ray transitions of the evaporation residues (ERs)  ${}^{96-98}\text{Ru}$  and  ${}^{97}\text{Tc}$  are labeled in Fig. 1(a). The cross sections of  ${}^{96-98}\text{Ru}$  and  ${}^{97}\text{Tc}$  were obtained using the in-beam method taking the level schemes from Refs. [14–16]. The cross sections for  ${}^{97}\text{Ru}$  were also extracted using the off-beam  $\gamma$ -ray counting method and found to be consistent with the in-beam measurements and with the values reported in Ref. [17]. The weighted average values of the cross sections obtained from the in-beam and off-beam methods are shown in Fig. 3(c). The cross sections for  ${}^{96,98}\text{Ru}$  and  ${}^{97}\text{Tc}$  are plotted in the same figure.

## IV. CALCULATIONS

Statistical model calculations were carried out using the code PACE [18] to estimate the contribution from complete fusion to the residues resulting from  $\alpha$  and  $t$  capture. The angular momentum distribution obtained from the coupled-channel code CCFULL [19] was used as input at each energy to obtain the cross sections of the decay channels. The estimated ER cross sections explain the measured values as shown in Fig. 3(c). The calculated cross sections for  ${}^{94,95}\text{Mo}$  are found to be smaller by an order of magnitude relative

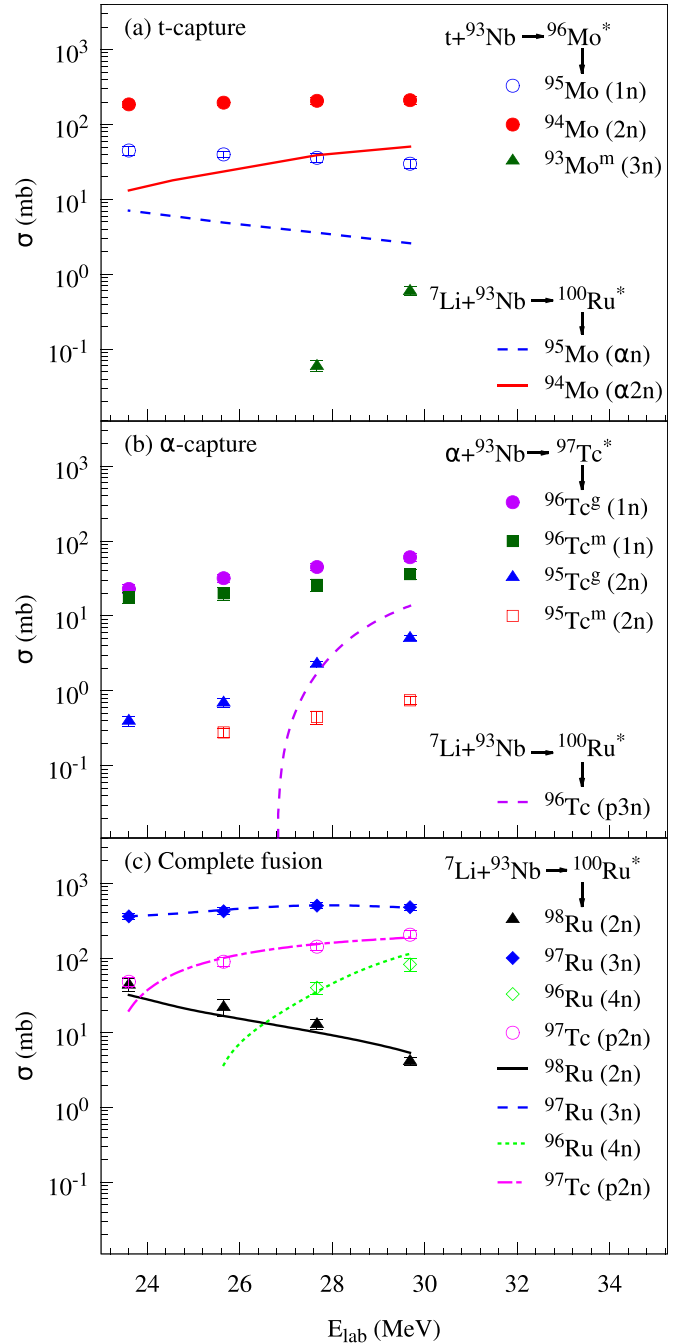


FIG. 3. The measured cross sections for residues arising from  $t$ -capture,  $\alpha$ -capture and CF for the  ${}^7\text{Li} + {}^{93}\text{Nb}$  reaction. (a) The cross sections for  ${}^{93,94,95}\text{Mo}$  nuclei are denoted by filled triangles, filled circles, and open circles, respectively. (b) The filled triangles, open boxes, filled circles, and filled boxes correspond to the cross sections for the ground states and isomeric states of  ${}^{95,96}\text{Tc}$ , respectively. (c) The cross sections for the  $2n$ ,  $3n$ ,  $4n$ , and  $p2n$  evaporation channels following CF are denoted by filled triangles, open diamonds, filled diamonds, and open circles, respectively. The lines are the statistical model (PACE) estimates for the corresponding residues.

to the measured cross sections at all energies, as shown in Fig. 3(a). This observation suggests that the dominant reaction mechanism responsible for production of  ${}^{93-95}\text{Mo}$  nuclei is not compound nuclear fusion but  $t$  capture. Similarly, the predicted

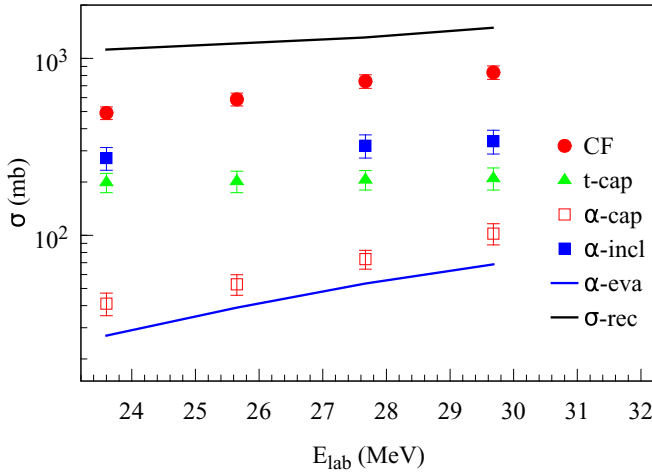


FIG. 4. The measured cross sections for  $t$  capture,  $\alpha$  capture, CF,  $\alpha$ -incl (from Ref. [6]) are denoted by filled triangles, open squares, filled circles, and filled squares, respectively. The dashed line is the estimated  $\alpha$ -evaporation cross section from the statistical model calculations. The calculated reaction cross sections from Ref. [6] are shown by the solid line.

cross sections for  $^{96}\text{Tc}$  are found to be far smaller than the measured values, implying that  $^{95,96}\text{Tc}$  nuclei are produced mainly by the  $\alpha$ -capture mechanism. The cross sections of individual residues from  $\alpha$  and  $t$  capture were corrected for the contribution from the compound nucleus. The  $t$ -capture,  $\alpha$ -capture, and complete fusion cross sections were obtained by taking the sum of individual residue cross sections and are presented in Fig. 4. The cross sections for  $t$  capture are found to be larger than those for  $\alpha$  capture at all energies, in agreement with the results reported in earlier studies with  $^7\text{Li}$  projectiles [10,20,21]. The estimated  $\alpha$ -particle evaporation cross sections are also plotted in Fig. 4 as well as the calculated reaction cross sections from Ref. [6].

The  $^{93}\text{Nb}(^7\text{Li}, ^5\text{He})^{95}\text{Mo}$  and  $^{93}\text{Nb}(^7\text{Li}, ^6\text{He})^{94}\text{Mo}$  stripping processes may also contribute to the production of  $^{93-95}\text{Mo}$  nuclei. A meaningful estimate of the  $d$ -stripping cross section is not possible due to the lack of suitable nuclear structure information concerning the  $\langle ^{95}\text{Mo} | ^{93}\text{Nb} + d \rangle$  overlaps. However, an estimate of the  $p$ -stripping cross section was made through distorted wave Born approximation calculations

performed using the code FRESKO [22]. The entrance channel optical potentials used the global  $^7\text{Li}$  parameters of Ref. [23] which give a satisfactory description of the elastic scattering data of Ref. [6]. The exit channel potentials employed the global  $^6\text{Li}$  parameters of Ref. [23], the comparative study of Ref. [24] suggesting that for a  $^{94}\text{Mo}$  target at these energies the  $^6\text{Li}$  optical potentials should describe  $^6\text{He}$  elastic scattering equally well. The  $\langle ^7\text{Li} | ^6\text{He} + p \rangle$  overlaps were calculated with the transferred  $p$  bound in a Woods-Saxon well of radius  $1.25 \times 6^{1/3}$  fm and diffuseness 0.65 fm with a spin-orbit term of Thomas form and depth 6 MeV, the depth of the central part being adjusted to give the correct binding energy. The spectroscopic factor was taken from Ref. [25]. The  $\langle ^{94}\text{Mo} | ^{93}\text{Nb} + p \rangle$  overlaps were taken from the  $^{93}\text{Nb}(^3\text{He}, d)$  study of Ref. [26] and transfers to all the  $^{94}\text{Mo}$  states in Table VIII of that work were included in the calculations. The estimated cross sections for  $p$  stripping are  $\sim 2$  mb at the incident  $^7\text{Li}$  energies studied here. This value will be something of a lower limit since the optimum  $Q$  value for this reaction is about  $-8$  MeV, favoring population of  $^{94}\text{Mo}$  levels at about 6.5 MeV, whereas the maximum excitation energy of the  $^{94}\text{Mo}$  states included in the calculations was  $\sim 3$  MeV. We may estimate the actual values to be around a few mb (i.e., less than 10 mb). The  $d$  stripping cross section is expected to be smaller than that for  $p$  stripping, from the semiclassical trajectory matching condition. Thus, neither process is expected to contribute significantly to the observed Mo residue cross sections.

## V. DISCUSSION

The cross sections of all important reaction mechanisms contributing to the  $\alpha$  yield [as seen in Fig. 1(b)] from the present measurement and earlier work [6] are listed in Table I for comparison. The statistical model predictions for  $\alpha$ -particle evaporation ( $\sigma_{\alpha}^{\text{CN}}$ ) from the compound nucleus are also given. The  $t$ -capture process is found to be the dominant reaction mechanism, which accounts for  $\sim 62-73\%$  of  $\sigma_{\alpha}^{\text{incl}}$ , whereas the combined contribution of the breakup and nucleon transfer followed by breakup channels is  $\sim 15\%$ . The cumulative contributions from all these measured reaction processes and estimated CN contribution are also tabulated in Table I, which explain  $\sim 95\%$  of the measured  $\sigma_{\alpha}^{\text{incl}}$ .

TABLE I. The cross sections of all possible reaction mechanisms contributing to the  $\alpha$ -particle yield.  $t$  capture:  $\sigma_{t\text{-cap}}$ ,  $2n$  stripping ( $^7\text{Li}, ^5\text{Li} \rightarrow \alpha + p$ )  $^{95}\text{Nb}$ :  $\sigma_{\alpha}^{\alpha-p}$ , inelastic excitation ( $^7\text{Li}, ^7\text{Li}^* \rightarrow \alpha + t$ )  $^{93}\text{Nb}$ :  $\sigma_{\alpha}^{\alpha-t}$ ,  $1n$  stripping ( $^7\text{Li}, ^6\text{Li}^* \rightarrow \alpha + d$ )  $^{94}\text{Nb}$ :  $\sigma_{\alpha}^{\alpha-d}$ ,  $1p$  pickup ( $^7\text{Li}, ^8\text{Be} \rightarrow \alpha + \alpha$ )  $^{92}\text{Zr}$ :  $\sigma_{\alpha}^{\alpha-\alpha}$ , and  $\alpha$ -particle evaporation from the compound nucleus estimated using the code PACE:  $\sigma_{\alpha}^{\text{CN}}$  are presented. The cumulative contribution  $\sigma_{\alpha}^{\text{total}}$  along with the inclusive  $\alpha$  yield ( $\sigma_{\alpha}^{\text{incl}}$ ) from Ref. [6] are also given.

$E_{\text{lab}}$ (MeV)	$\sigma_{t\text{-cap}}$ (mb)	$\sigma_{\alpha}^{\alpha-p}$ (mb)	$\sigma_{\alpha}^{\alpha-t}$ (mb)	$\sigma_{\alpha}^{\alpha-d}$ (mb)	$\sigma_{\alpha}^{\alpha-\alpha}$ (mb)	$\sigma_{\alpha}^{\text{CN}}$ (mb)	$\sigma_{\alpha}^{\text{total}}$ (mb)	$\sigma_{\alpha}^{\text{incl}}$ (mb)	$\sigma_{\alpha}^{\text{total}}/\sigma_{\alpha}^{\text{incl}}$ (%)
23.6	$199 \pm 34$	$17.3 \pm 3.0$	$15.1^{\text{b}} \pm 1.4$	$5.2 \pm 0.5$	$2.0 \pm 0.2$	27	$266 \pm 39$	$273 \pm 40$	97
25.6	$202 \pm 37$	$17.5 \pm 2.8$	$15.9^{\text{b}} \pm 1.4$	$5.5^{\text{a}} \pm 0.5$	$2.2^{\text{a}} \pm 0.2$	39	$282 \pm 42$	$296^{\text{a}} \pm 50$	95
27.7	$206 \pm 33$	$20.1 \pm 2.5$	$16.8 \pm 1.2$	$5.8 \pm 0.4$	$2.6 \pm 0.2$	53	$304 \pm 38$	$321 \pm 48$	95
29.7	$210 \pm 35$	$18.8 \pm 3.0$	$18.0^{\text{b}} \pm 1.2$	$6.2 \pm 0.4$	$3.0 \pm 0.4$	69	$325 \pm 41$	$340 \pm 52$	96

<sup>a</sup>Interpolated value.

<sup>b</sup>Extrapolated value.

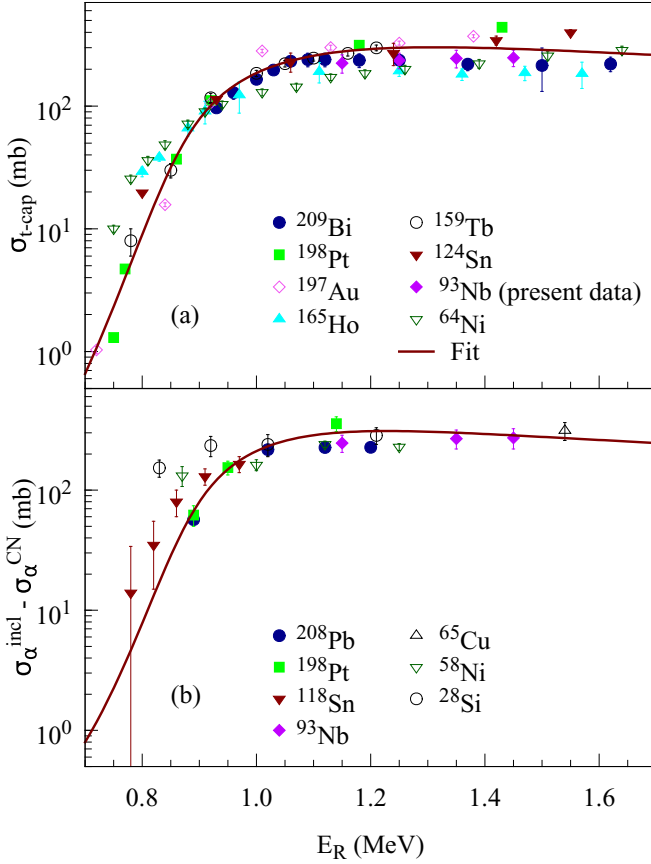


FIG. 5. (a)  $t$ -capture and (b) inclusive  $\alpha$ -production cross sections after the subtraction of the compound nuclear contribution, for  ${}^7\text{Li}$  projectiles incident on several targets including  ${}^{93}\text{Nb}$  (present data) as a function of  $E_R = E_{\text{c.m.}}/[Z_p Z_t/(A_p^{1/3} + A_t^{1/3})]$ . The solid lines represent the best fit to the  $t$ -capture data.

A systematic study of the  $t$ -capture and inclusive  $\alpha$  cross sections was carried out for reactions involving  ${}^7\text{Li}$  over a range of lighter to heavier targets including the present system. The measured  $\sigma_{t\text{-cap}}$  for the  ${}^7\text{Li} + {}^{93}\text{Nb}$  (present work),  ${}^7\text{Li} + {}^{209}\text{Bi}$  [20],  ${}^7\text{Li} + {}^{197}\text{Au}$  [27],  ${}^7\text{Li} + {}^{198}\text{Pt}$  [10],  ${}^7\text{Li} + {}^{165}\text{Ho}$  [28],  ${}^7\text{Li} + {}^{159}\text{Tb}$  [29],  ${}^7\text{Li} + {}^{124}\text{Sn}$  [30], and  ${}^7\text{Li} + {}^{64}\text{Ni}$  [31] systems are presented in Fig. 5(a). The  $x$  axis in Fig. 5 is defined as  $E_R = E_{\text{c.m.}}/[Z_p Z_t/(A_p^{1/3} + A_t^{1/3})]$ , where  $E_{\text{c.m.}}$ ,  $Z_p$ ,  $Z_t$ ,  $A_p$ ,  $A_t$  are the beam energy in the center of mass frame,  ${}^7\text{Li}$  and target atomic numbers,  ${}^7\text{Li}$  and target mass numbers, respectively. The  $\sigma_{t\text{-cap}}$  are found to follow the Wong formula [32], slightly modified to obtain a better fit at energies above the Coulomb barrier:

$$\sigma_{t\text{-cap}} = \frac{ac}{2x} \ln \left[ 1 + \exp \left\{ \frac{2\pi}{c} (d - b) \tanh \left( \frac{x - b}{d - b} \right) \right\} \right], \quad (1)$$

where  $x = E_R$ , and  $a$ ,  $b$ ,  $c$ , and  $d$  are adjustable parameters.

The inclusive  $\alpha$  cross sections ( $\sigma_{\alpha}^{\text{incl}}$ ) after subtraction of the compound nuclear component ( $\sigma_{\alpha}^{\text{CN}}$ ) estimated using the statistical model code PACE for the  ${}^7\text{Li} + {}^{208}\text{Pb}$  [33],  ${}^7\text{Li} + {}^{198}\text{Pt}$  [34],  ${}^7\text{Li} + {}^{118}\text{Sn}$  [35],  ${}^7\text{Li} + {}^{93}\text{Nb}$  [6],  ${}^7\text{Li} + {}^{65}\text{Cu}$  [36],  ${}^7\text{Li} + {}^{58}\text{Ni}$  [35], and  ${}^7\text{Li} + {}^{28}\text{Si}$  [37] systems are pre-

sented in Fig. 5(b). The curve obtained after fitting  $\sigma_{t\text{-cap}}$  is replotted in Fig. 5(b) as the solid line and is found to explain the general trend observed for  $\sigma_{\alpha}^{\text{incl}} - \sigma_{\alpha}^{\text{CN}}$  as well. This observation also suggests that the main contribution to  $\sigma_{\alpha}^{\text{incl}}$  is  $\sigma_{t\text{-cap}}$ . For the light mass targets  ${}^{12}\text{C}$ ,  ${}^{27}\text{Al}$ , and  ${}^{28}\text{Si}$  [37–39], there is a substantial contribution from  $\alpha$ -particle evaporation from the compound nucleus. However, for the heavier targets the  $t$ -capture mechanism is the main source of  $\alpha$ -particle production. For  ${}^6\text{Li}$   $d$  capture is reported to be the dominant mechanism of  $\alpha$  production [2,35,40,41].

## VI. SUMMARY AND CONCLUSIONS

In summary, the origin of the large inclusive  $\alpha$  cross sections for the  ${}^7\text{Li} + {}^{93}\text{Nb}$  system at energies around the Coulomb barrier was investigated. The reaction processes leading to  $\alpha$  particles in the exit channels were identified using particle- $\gamma$  coincidence measurements. The relative yields of  $\gamma$  rays from the residues of  $t$  capture were found to be greater than those from the other processes. The absolute cross sections for  $t$  capture,  $\alpha$  capture, and  $2n$  stripping along with the complete fusion were also measured using the in-beam and off-beam  $\gamma$ -ray counting methods. Statistical model calculations were performed to estimate the compound nuclear contribution to the cross sections of residues populated in  $t$ -capture and  $\alpha$ -capture reactions. The measured  $t$ -capture cross sections are found to be greater than the  $\alpha$ -capture cross sections at all energies. The present study shows that the  $t$ -capture mechanism is the dominant reaction channel for the production of  $\alpha$  particles and accounts for 62–73% of the measured inclusive  $\alpha$  cross sections. The  $2n$  stripping ( ${}^5\text{Li} \rightarrow \alpha + p$ ) cross sections together with earlier data on the  $1p$  pickup ( ${}^8\text{Be} \rightarrow \alpha + \alpha$ ), inelastic excitation ( ${}^7\text{Li}^* \rightarrow \alpha + t$ ), and  $1n$  stripping ( ${}^6\text{Li}^* \rightarrow \alpha + d$ ) from Ref. [6] explain  $\sim 15\%$  of the inclusive  $\alpha$  cross sections. The statistical model predictions of the compound nuclear contributions from  $\alpha$ -evaporation account for 10–20% of the inclusive  $\alpha$  cross sections. The combination of  $\alpha$  production due to: (a)  $t$  capture, (b) evaporation from the compound nucleus, and (c) breakup and nucleon transfer followed by breakup, explains almost all the measured inclusive  $\alpha$  cross sections for the  ${}^7\text{Li} + {}^{93}\text{Nb}$  system over the measured energy range. The present measurements, together with a systematic study of  $t$  capture and inclusive  $\alpha$  cross sections for different systems, suggest that the main  $\alpha$ -production mechanism is  $t$  capture, although at present it is still not possible to say exactly how the capture takes place. An analysis of the present complete data set on  $\alpha$  production using stochastic breakup and other model calculations [4,42,43] could shed light on whether the observed  $t$  capture is a direct and/or two-step process.

## ACKNOWLEDGMENTS

We thank the Mumbai Pelletron-Linac accelerator staff for providing a steady and uninterrupted beam and Mr. P. Patale for help during the experiment.

- [1] N. Keeley, N. Alamanos, K. W. Kemper, and K. Rusek, *Prog. Part. Nucl. Phys.* **63**, 396 (2009).
- [2] L. F. Canto, P. R. S. Gomes, R. Donangelo, J. Lubian, and M. Hussein, *Phys. Rep.* **596**, 1 (2015).
- [3] J. J. Kolata, V. Guimares, and E. F. Aguilera, *Eur. Phys. J. A* **52**, 123 (2016).
- [4] J. Lei and A. M. Moro, *Phys. Rev. C* **95**, 044605 (2017).
- [5] O. Sgouros, A. Pakou, D. Pierroutsakou, M. Mazzocco, L. Acosta, X. Aslanoglou, C. Betsou, A. Boiano, C. Boiano, D. Carbone, M. Cavallaro, J. Grebosz, N. Keeley, M. La Commara, C. Manea, G. Marquinez-Duran, I. Martel, N. G. Nicolis, C. Parascandolo, K. Rusek, A. M. Sánchez-Benítez, C. Signorini, F. Soramel, V. Soukeras, C. Stefanini, E. Stiliaris, E. Strano, I. Strojek, and D. Torresi, *Phys. Rev. C* **94**, 044623 (2016).
- [6] S. K. Pandit, A. Shrivastava, K. Mahata, N. Keeley, V. V. Parkar, P. C. Rout, K. Ramachandran, I. Martel, C. S. Palshetkar, A. Kumar, A. Chatterjee, and S. Kailas, *Phys. Rev. C* **93**, 061602(R) (2016).
- [7] C. M. Castaneda, H. A. Smith, Jr., P. Singh, J. Jastrzebski, H. Karwowski, and A. Gaigalas, *Phys. Lett. B* **77**, 371 (1978).
- [8] H. Utsunomiya, S. Kubono, M. H. Tanaka, M. Sugitani, K. Morita, T. Nomura, and Y. Hamajima, *Phys. Rev. C* **28**, 1975 (1983).
- [9] V. Tripathi, A. Navin, V. Nanal, R. G. Pillay, K. Mahata, K. Ramachandran, A. Shrivastava, A. Chatterjee, and S. Kailas, *Phys. Rev. C* **72**, 017601 (2005).
- [10] A. Shrivastava, A. Navin, A. Diaz-Torres, V. Nanal, K. Ramachandran, M. Rejmund, S. Bhattacharyya, A. Chatterjee, S. Kailas, A. Lemasson, R. Palit, V. V. Parkar, R. Pillay, P. C. Rout, and Y. Sawant, *Phys. Lett. B* **718**, 931 (2013).
- [11] R. Palit, S. Saha, J. Sethi, T. Trivedi, S. Sharma, B. Naidu, S. Jadhav, R. Donthi, P. Chavan, H. Tan, and W. Hennig, *Nucl. Instrum. Methods Phys. Res. A* **680**, 90 (2012).
- [12] B. Kharraja, S. S. Ghugre, U. Garg, R. V. F. Janssens, M. P. Carpenter, B. Crowell, T. L. Khoo, T. Lauritsen, D. Nisius, W. Reviol, W. F. Mueller, L. L. Riedinger, and R. Kaczarowski, *Phys. Rev. C* **57**, 2903 (1998).
- [13] J. M. Chatterjee, M. Saha-Sarkar, S. Bhattacharya, S. Sarkar, R. P. Singh, S. Murulithar, and R. K. Bhowmik, *Phys. Rev. C* **69**, 044303 (2004).
- [14] B. Kharraja, S. S. Ghugre, U. Garg, R. V. F. Janssens, M. P. Carpenter, B. Crowell, T. L. Khoo, T. Lauritsen, D. Nisius, W. Reviol, W. F. Mueller, L. L. Riedinger, and R. Kaczarowski, *Phys. Rev. C* **57**, 83 (1998).
- [15] R. Broda, M. Ishihara, B. Herskind, H. Oeschler, S. Ogaza, and H. Ryde, *Nucl. Phys. A* **248**, 356 (1975).
- [16] D. Hippe, H. W. Schuh, U. Kaup, K. O. Zell, P. von Brentano, and D. B. Fossan, *Z. Phys., A* **311**, 329 (1983).
- [17] D. Kumar, M. Maiti, and S. Lahiri, *Phys. Rev. C* **94**, 044603 (2016).
- [18] A. Gavron, *Phys. Rev. C* **21**, 230 (1980).
- [19] K. Hagino, N. Rowley, and A. Kruppa, *Comput. Phys. Commun.* **123**, 143 (1999).
- [20] M. Dasgupta, P. R. S. Gomes, D. J. Hinde, S. B. Moraes, R. M. Anjos, A. C. Berriman, R. D. Butt, N. Carlin, J. Lubian, C. R. Morton, J. O. Newton, and A. Szanto de Toledo, *Phys. Rev. C* **70**, 024606 (2004).
- [21] V. V. Parkar, V. Jha, and S. Kailas, *Phys. Rev. C* **94**, 024609 (2016).
- [22] I. J. Thompson, *Comput. Phys. Rep.* **7**, 167 (1988).
- [23] J. Cook, *Nucl. Phys. A* **388**, 153 (1982).
- [24] Y. Kucuk, I. Boztosun, and N. Keeley, *Phys. Rev. C* **79**, 067601 (2009).
- [25] S. Cohen and D. Kurath, *Nucl. Phys. A* **101**, 1 (1967).
- [26] M. R. Cates, J. B. Ball, and E. Newman, *Phys. Rev.* **187**, 1682 (1969).
- [27] C. S. Palshetkar, S. Thakur, V. Nanal, A. Shrivastava, N. Dokania, V. Singh, V. V. Parkar, P. C. Rout, R. Palit, R. G. Pillay, S. Bhattacharyya, A. Chatterjee, S. Santra, K. Ramachandran, and N. L. Singh, *Phys. Rev. C* **89**, 024607 (2014).
- [28] V. Tripathi, A. Navin, K. Mahata, K. Ramachandran, A. Chatterjee, and S. Kailas, *Phys. Rev. Lett.* **88**, 172701 (2002).
- [29] A. Mukherjee, S. Roy, M. Pradhan, M. S. Sarkar, P. Basu, B. Dasmahapatra, T. Bhattacharya, S. Bhattacharya, S. Basu, A. Chatterjee, V. Tripathi, and S. Kailas, *Phys. Lett. B* **636**, 91 (2006).
- [30] V. V. Parkar *et al.* [Phys. Rev. C (to be published)].
- [31] Md. Moin Shaikh, S. Roy, S. Rajbanshi, A. Mukherjee, M. K. Pradhan, P. Basu, V. Nanal, S. Pal, A. Shrivastava, S. Saha, and R. G. Pillay, *Phys. Rev. C* **93**, 044616 (2016).
- [32] C. Y. Wong, *Phys. Rev. Lett.* **31**, 766 (1973).
- [33] C. Signorini, M. Mazzocco, G. Prete, F. Soramel, L. Stroe, A. Andrighetto, I. Thompson, A. Vitturi, A. Brondi, M. Cinausero, D. Fabris, E. Fioretto, N. Gelli, J. Guo, G. La Rana, Z. Liu, F. Lucarelli, R. Moro, G. Nebbia, M. Trotta, E. Vardaci, and G. Viesti, *Eur. Phys. J. A* **10**, 249 (2001).
- [34] S. K. Pandit *et al.* (to be published).
- [35] K. Pfeiffer, E. Speth, and K. Bethge, *Nucl. Phys. A* **206**, 545 (1973).
- [36] A. Shrivastava, A. Navin, N. Keeley, K. Mahata, K. Ramachandran, V. Nanal, V. V. Parkar, A. Chatterjee, and S. Kailas, *Phys. Lett. B* **633**, 463 (2006).
- [37] A. Pakou, N. G. Nicolis, K. Rusek, N. Alamanos, G. Doukelis, A. Gillibert, G. Kalyva, M. Kokkoris, A. Lagoyannis, A. Musumarra, C. Papachristodoulou, G. Perdikakis, D. Pierroutsakou, E. C. Pollacco, A. Spyrou, and C. Zarkadas, *Phys. Rev. C* **71**, 064602 (2005).
- [38] V. V. Parkar, K. Mahata, S. Santra, S. Kailas, A. Shrivastava, K. Ramachandran, A. Chatterjee, V. Jha, and P. Singh, *Nucl. Phys. A* **792**, 187 (2007).
- [39] K. Kalita, S. Verma, R. Singh, J. J. Das, A. Jhingan, N. Madhavan, S. Nath, T. Varughese, P. Sugathan, V. V. Parkar, K. Mahata, K. Ramachandran, A. Shrivastava, A. Chatterjee, S. Kailas, S. Barua, P. Basu, H. Majumdar, M. Sinha, R. Bhattacharya, and A. K. Sinha, *Phys. Rev. C* **73**, 024609 (2006).
- [40] C. Signorini, A. Edifizi, M. Mazzocco, M. Lunardon, D. Fabris, A. Vitturi, P. Scopel, F. Soramel, L. Stroe, G. Prete, E. Fioretto, M. Cinausero, M. Trotta, A. Brondi, R. Moro, G. La Rana, E. Vardaci, A. Ordine, G. Inghima, M. La Commara, D. Pierroutsakou, M. Romoli, M. Sandoli, A. Diaz-Torres, I. J. Thompson, and Z. H. Liu, *Phys. Rev. C* **67**, 044607 (2003).
- [41] S. Santra, S. Kailas, V. V. Parkar, K. Ramachandran, V. Jha, A. Chatterjee, P. K. Rath, and A. Parihari, *Phys. Rev. C* **85**, 014612 (2012).
- [42] A. Diaz-Torres, D. J. Hinde, J. A. Tostevin, M. Dasgupta, and L. R. Gasques, *Phys. Rev. Lett.* **98**, 152701 (2007).
- [43] M. Boselli and A. Diaz-Torres, *Phys. Rev. C* **92**, 044610 (2015).